Stabilization effects of Mn(II)-salts on metaschoepite in soil under different water regimes

Fuyu Guo[a,b,c], Georgio Proctor[b], Steven L. Larson[d] , John H. Ballard[d], Heather M. Knotek-Smith[d], Dongmei Cao[e], Ruyi Yang[a], Xingxiang Wang[c], Fengxiang Han[b*]

[a] School of Ecology and Environment, Anhui Normal University, Wuhu 241002, China

[b] Department of Chemistry, Physics and Atmospheric Sciences, Jackson State University, Jackson, MS 39217, USA

[c] Institute of Soil Science, Chinese Academy of Sciences, Nanjing 210008, China

[d] U.S. Army Engineer Research and Development Center, 3909 Halls Ferry Rd., Vicksburg, MS 39180-6199, USA.

[e] Shared Instrument Facility, Louisiana State University, Baton Rouge, LA 70803, USA

*Corresponding author: Fengxiang Han (Fengxiang.han@jsums.edu)

ABSTRACT

Metaschoepite ($UO_3 \cdot 2H_2O$) is a product of the corrosion of depleted uranium munition and commonly found in former war zones and at military test sites. Understanding metaschoepite transformation and uranium (U) mobility is important for sustainable operation of U containing test-firing and nuclear waste disposal sites. In the present study, the stabilization effects of Mn(II)-salts on metaschoepite in soil under different water regimes (saturation and flooding) were investigated. Results indicated that the dissolution and transformation of metaschoepite were controlled by water regimes and redox processes in soil system. The concentrations of water-extractable U in the metaschoepite-amended soils after 270 days' incubation for the saturation and flooding groups were 299 and 173 mg kg^{-1}, respectively. The addition of Mn(II)-salts significantly retarded the releasing of U(VI) in the metaschoepite-amended soils. The U stabilization efficiency of Mn(II) were persistently > 90% during 270 days' incubation, irrespective of water regimes. The X-ray photoelectron spectroscopy results showed no detectable reduction of liberated U(VI) in the "open waterlogged" soil system, while the X-ray diffraction analyses confirmed the transformation of metaschoepite with signals of schoepites disappearing over the course of the experiment. The study highlights the potential for the use of Mn(II)-salts in practical application for in-situ stabilization of U-contaminated sites and nuclear waste disposal.

KEYWORDS: Metaschoepite, Mn(II)-chloride, Saturation, Flooding, Stabilization efficiency

1. INTRODUCTION

Uranium (U) is a ubiquitous metallic element in the natural environment. Natural uranium is a mixture of three radioactive isotopes at percentages of approximately 99.27% ^{238}U, 0.72% ^{235}U, and 0.0054% ^{234}U, respectively.[1] Depleted uranium (DU) is a by-product of nuclear fuel enrichment that it is depleted in ^{235}U and ^{234}U. The high density of depleted uranium (19 g cm^{-3}) make it useful for a range of civilian and military activities.[2] Soil contaminated with DU has found to be associated with distributive uses of depleted uranium such as the use of DU penetrators during wars in Kosovo, Kuwait, Iraq and in Syria. Military testing and training areas where DU ammunition is used can have elevated levels of uranium in soils.[3, 4] In the U.S., testing and training activities using DU kinetic energy penetrator munitions have resulted in DU containing soils at a number of facilities. One such site, Yuma Proving Grounds, in western Arizona is a general-purpose desert environment test facility that has conducted test firing of DU weapons since the 1980s with an area of approximately 1200 acres.[5]

The metallic form of DU is prone to oxidation and will corrode over time in natural systems. The oxidation, dissolution and recrystallization processes that can occur during the weathering of DU penetrators and penetrator fragments can result in the formation of soluble and crystalline phases such as schoepite ($UO_3 \cdot 2.25H_2O$), dehydrated schoepite ($UO_3 \cdot 0.75H_2O$) and metaschoepite ($UO_3 \cdot 2H_2O$) along with more complex minerals such as becquerelite and studtite.[6-8] A site study in the southwestern U.S. described residues around corroded DU penetrators as silica-cemented, mixed schoepite-metaschoepite/clay/silt aggregates, as schoepite/metaschoepite-only aggregates, or rarely as coatings upon soil grains.[9] A more recent study showed $UO_{2.8}$ and UO_3 to be present in the DU metallic fragment/soil systems in saturated soil regimes.[10] Soil moisture affected the rate of corrosion of DU fragments. DU metal corrosion rates decreased

following the trend: saturated soil > field moisture capacity soil > air dry soil. The corrosion or dissolution of DU occurs when the U(IV) oxidation products of the zero-valent U metal further oxidization of U(IV) oxide to U(VI) minerals.[5] The corrosion processes of DU penetrators have been shown to depend on soil biogeochemical conditions such as pH, Eh, soil chemical composition, and water moisture conditions.[8, 10, 11] The U(VI) solid phases in the schoepite family ($UO_3 \cdot nH_2O$) represent possible sources of more mobile uranium species in the dissolved or colloidal state.[7] A recent field study indicated schoepites ($UO_3 \cdot nH_2O$) were present as the major uranium containing mineral family at the Yuma Proving Weapon Testing sites.[3]

U occurs in a wide range of valence states. Two states predominate in near-surfaces environments: tetravalent uranium, U(IV), and hexavalent uranium, U(VI).[12] The mobility, solubility, and toxicity of U depend on the speciation and redox states, with reducing species being, in general, relatively more insoluble and immobile. Under oxidizing conditions, U is primarily present in its hexavalent state as uranyl cation (UO_2^{2+}), forming numerous aqueous complexes.[13, 14] However, under reducing conditions, U(IV), such as uraninite (UO_2) (log K_{sp} = -54.6), is the common species, which is sparingly soluble, less mobile and less bioavailable to plants compared to U(VI) species.[15, 16] The solubility of uraninite at near neutral pH is ~5 orders of magnitude lower than for metaschoepite (~10 mg L^{-1}).[17] Thus, reductive conversion of mobile U(VI) to immobile U(IV) is a desirable strategy for the retardation of U migration at sites with U soil contamination.

In natural environment, U(VI) can be reduced by several abiotic and microbially mediated processes. Lovley et al. reported that the dissimilatory Fe(III)-reducing microorganisms could obtain energy for growth by electron transport to U(VI),[18] and it was generally believed that abiotic processes such as U(VI) reduction by sulfide, Fe(II), or hydrogen were responsible for the presence of U(IV) in anaerobic or low redox environments. Recently, numerous studies have increasingly

78 focused on the abiotic sorption and reduction of uranyl on various Fe(II)-bearing materials, such
79 as iron sulfides[19] and iron salts.[20] Manganese (Mn) is the second transition metal and resembles Fe
80 in several aspects of its biogeochemistry, Mn oxide minerals are ubiquitous in natural
81 environments as coatings and fine-grained aggregates that play important roles in elements'
82 biogeochemical cycles.[21] With large specific surface areas and powerful oxidizing activity,
83 manganese oxides can influence the fate and transport of U in soil and groundwater.[22] Wang et al.
84 investigated the adsorption of U(VI) to synthetic and biogenic MnO_2, and found that the uranium
85 species present on the synthetic δ-MnO_2 surfaces is predominated by $(\equiv MnO)_2UO_2$ in the pH
86 range 2-8, and $\equiv MnOUO_2(OH)_2^-$ and $(\equiv MnO)_2UO_2(CO_3)_2^{4-}$ at pH 8 and above.[23] Ren et al.
87 synthesized a series of Mn oxide materials of different structures (α-MnO_2, γ-MnO_2, δ-MnO_2,
88 Mn_3O_4, MnOOH) and found that α-MnO_2 showed the largest uranium uptake at 280 mg g^{-1}.[24] Lee
89 et al. synthesized a number of nanocrystalline forms of MnO_2 for a study of uranium sorption and
90 separation that showed uranyl sorption capacities as high as 600 mg g^{-1}.[25] While manganese oxides
91 can retard U transport in the subsurface, they also can oxidize U(IV) species to more soluble U(VI)
92 species, potentially remobilizing U. Liu et al. found that the overall rate of U(VI) reduction in
93 dissimilatory metal-reducing bacteria suspensions was decreased by the presence of the Mn(IV)
94 oxide, pyrolusite (β-MnO_2).[26] Therefore, in natural environment, the coupling of the
95 biogeochemical cycles of uranium and manganese may affect the fate and transport of U.

96 Reduction, sorption, or incorporation reactions involving the oxidation products from DU
97 penetrators and fragments in soils may limit U migration in the environment. The environmental
98 phenomena of the predominant U oxide mineral found in some firing range soils (metaschoepite,
99 $UO_3 \cdot 2H_2O$), and the role that metaschoepite plays in U transport under various biogeochemical
100 conditions is not well defined. The present study investigates the stabilization effects of Mn(II)-

salts on metaschoepite ($UO_3 \cdot 2H_2O$) in soil under different water regimes. The specific objectives were to: (1) explore the dissolution behavior of metaschoepite in soil under specific environmental conditions (i.e., saturation and flooding); (2) assess the effectiveness of in situ chemical stabilization of liberated U(VI) from metaschoepite using Mn(II)-salts.

2. MATERIALS AND METHODS

2.1 Soil and Metaschoepite

Soil collected from the Yuma Proving Ground (YPG), in southwestern La Paz county and western Yuma county in southwestern Arizona, U.S. from a non-DU impacted area was used as the clean-soil and the soil used to produce a metaschoepite contaminated (spiked) soil. The clean/pre-spiked soil samples were air-dried, homogenized and passed through a 10-mesh sieve. Soil samples taken from a highly impacted site at YPG were used as a source for the metaschoepite material. Individual metaschoepite containing particles (observable by their bright yellow color) (Fig. S1, S2) with minor becquerelite were individually removed from the highly contaminated soil samples. Schoepites and becquerelite were predominated products of the corrosion of DU ammunition in former war zones and weapon testing ranges,[3, 8, 9, 11, 27, 28] and in soil incubation experiments in the lab.[10, 29] The metaschoepite samples were crushed, and sieved to < 25 μm prior to use. The general soil properties and heavy metal concentrations of the clean-soil and metaschoepite are shown in Table 1.

Table 1

The selected physicochemical properties of the clean-soil and heavy metal concentrations of the clean-soil and metaschoepite

Parameters	Clean-soil	Metaschoepite
Texture（%）		
Gravel	2.3	
Sand	82.6	
Fines	15.1	
pH	8.76	
Total organic carbon (%)	0.014	
Electrical conductivity (μS cm^{-1})	7.91	
Cation exchange capacity (cmol kg^{-1})	0.215	
Fe (mg kg^{-1})	575 ± 89	2121 ± 233
Mn (mg kg^{-1})	133 ± 21	10762 ± 594
Cu (mg kg^{-1})	6.12 ± 0.12	102089 ± 4112
Zn (mg kg^{-1})	12.36 ± 1.11	15463 ±1983
Cr (mg kg^{-1})	6.43 ± 0.76	204 ± 51
Pb (mg kg^{-1})	3.22 ± 0.22	N.D.
U (mg kg^{-1})	2.51 ± 0.47	150392 ± 4768

Note: N.D., not detected. Values are means ± standard deviation (n = 3).

2.2 Experiment setup and sampling

An incubation experiment was conducted to investigate the stabilization effects of Mn(II)-salts on metaschoepite under different soil water content. Two water regimes were set: (i) saturation (S) and (ii) flooding (F). In the summer season, even though in high desert regions of YPG, a large amount of storms occurs often with severe flooding in the landscape. Therefore, the long-term effect of real summer stormy flooding scenario was simulated in this study.

The soil was saturated with deionized water, and the water content of 25% bring the clean-soil to the saturated paste state.[30] To simulate flooding, deionized water was added to form a 2-3 cm water layer covering the soil surface.[31] The water content of the flooded sample was approximately 40%. Three treatments performed for the saturated and flooded groups, referred to as CK, M, M+Mn. Each treatment used bottles with 150 g of soil. The CK was clean-soil without amendments, M was clean-soil with metaschoepite at 10% (w/w), and M+Mn was metaschoepite (10%, w/w) combined with Mn(II)-chloride (2%, w/w). The Mn(II)-chloride was purchased from the Fisher Scientific (analytical purity). Soils, metaschoepite and amendments were thoroughly blended[32] and placed into a wide mouth polypropylene bottle (diameter = 67 mm, height = 102 mm) in a randomized complete block design. Each treatment was performed in triplicate and the bottle caps perforated with holes to maintain the gas exchange. All bottles were incubated for 270 days in the dark. The loss of water (weighted) was supplemented every week using deionized water to maintain the water content.

During the incubation period, the soil pH and Eh values were measured in situ at time intervals of 1, 3, 7, 14, 30, 60, 90 and 270 d. Also, portions of soil (~10 g) were collected during the incubation period at 1, 30, 90, 270 d. The soil samples were freeze-dried, ground to pass through a 10-mesh sieve prior to the water extractable U and Mn analysis. At the end of the experiment (270 d), sub-soils were sampled using serum bottles with a butyl rubber stopper. The soils were immediately flash-frozen in liquid N_2 to preserve the soil matrix and then freeze-dried for the U and Mn species detection.

2.3 Analysis

The basic physicochemical characteristics of the clean-soil were determined according to the Methods of Soil Analysis. The pH of clean-soil was measured at a soil water ratio of 1:2.5 (w/v)

using a benchtop pH meter (Star A211, Thermo Scientific). The heavy metals in the clean-soil and metaschoepite were determined via the microwave-assisted (Multiwave GO, Anton Paar) acid digestion (9 mL HNO_3 + 3 mL HCl) according to the method EPA 3051A. The filtered digest solutions were analyzed using the inductively coupled plasma-mass spectrometry (ICP-MS, Agilent 7700). The certified reference soil sample (NIST SRM 2711a, Montana II soil) was used for quality control. During the incubation, the soil pH and Eh were measured in situ using a portable pH meter (Star A121, Thermo Scientific) and the Eh was measured using a Redox/ORP electrode (9179BNMD, Thermo Scientific).

Soils were extracted by deionized water for aqueous U and Mn concentration determination at time points of 1, 30, 90, 270 d.[33] Soil samples of 2.5 g were shaken on a reciprocal shaker at 200 rpm with 25 mL of deionized water for 2 h at room temperature. The suspensions were centrifuged at 5000 rpm for 10 min, filtered using a 0.45-μm membrane, and then acidified with 2 drops of 1 mol L^{-1} HNO_3. The U and Mn concentrations were analyzed using the inductively coupled plasma-optical emission spectrometry (ICP-OES, Optima 8000, PerkinElmer).

The dissolution and transformation behavior of metaschoepite as affected by Mn(II)-salts was tracked by X-ray power diffraction (XRD) and X-ray photoelectron spectroscopy (XPS). XRD analysis was conducted using a Rigaku-MiniFlex 600 diffractometer with CuKa irradiation (Ka = 1.54178 Å) at power settings of 40 kV and 35 mA. The XPS measurements were performed using a ScientaOmicron ESCA 2SR X-ray Photoelectron Spectroscope System equipped with a flood source charge neutralizer to determine the oxidation states of U and Mn in metaschoepite-amended soils. All analysis was carried out with a Mono Al Kα x-ray source (1486.6 eV) at the power of 450 W. A wide region survey scan and high-resolution core level scans of all elements were recorded and calibrated with the C1s 284.8ev as the reference peak. The core level spectra were

deconvoluted with CasaXPS software to obtain chemical state information. The surface morphology of metaschoepite was obtained through secondary electron imaging with a Tescan LYRA3 Scanning Electron Microscope (SEM).

2.4 Statistical analysis

All statistical analyses were carried out using the SPSS 22.0 (SPSS, IBM, USA). A two-way analysis of variance (ANOVA) was performed to test the main effects and interactions between incubation time and amendment treatments, and the Duncan's multiple range test (post hoc test) was used to assess the significant differences among amendment treatments. Data were expressed as the means ± standard deviation, and all figures were completed by the Origin 9.0 (Origin, OriginLab, USA). The U stabilization efficiency as affected by Mn(II)-salts was calculated as follows:

$$\text{Stabilization efficiency (\%)} = \frac{\text{Soluble U in control treatment} - \text{Soluble U in Mn treatment}}{\text{Soluble U in control treatment}} \times 100$$

3. RESULTS AND DISCUSSION

3.1 Dynamic changes of the soil pH and Eh

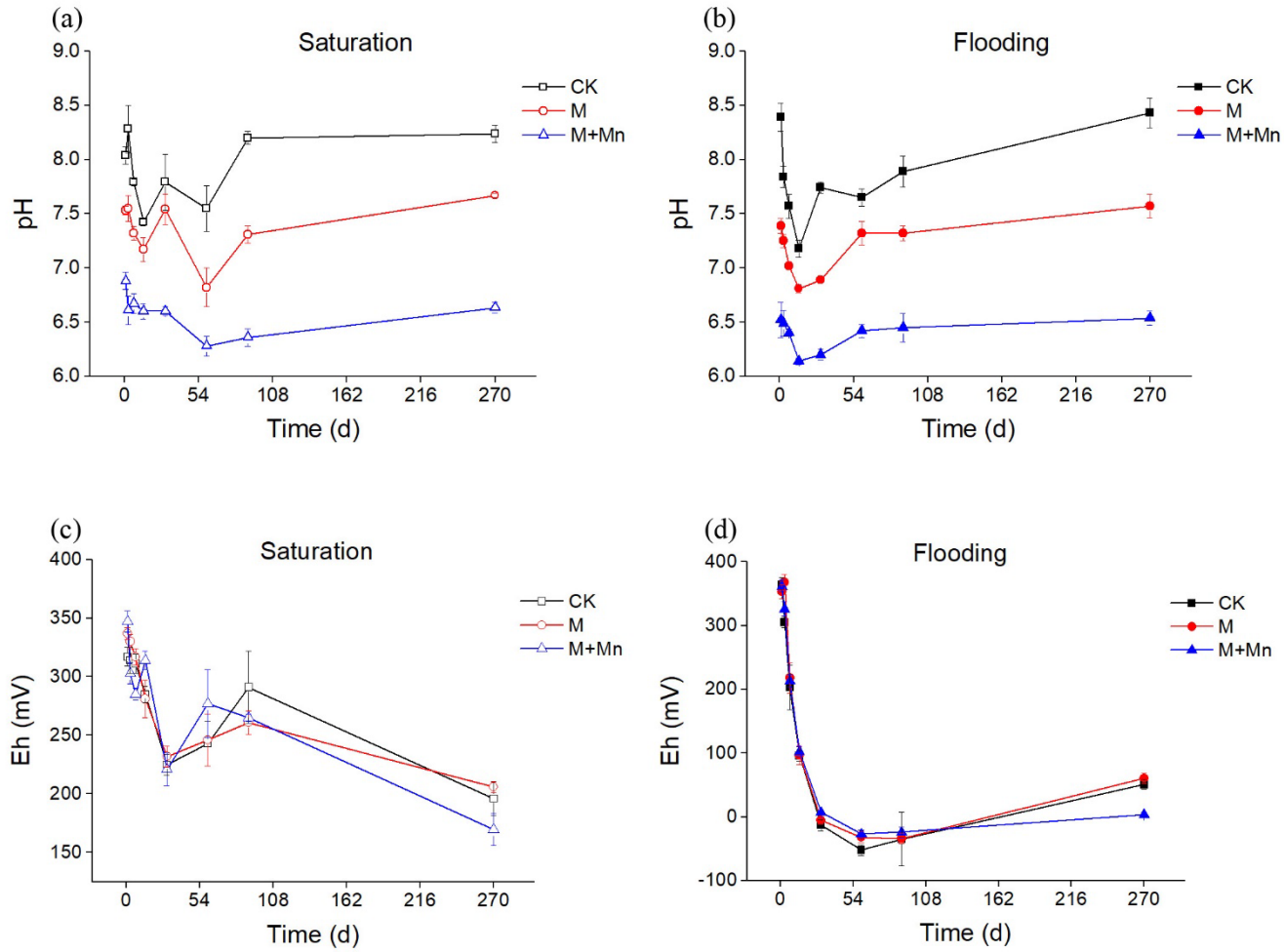

Fig 1. Dynamic changes of the pH and Eh during 270 d incubation. CK, clean-soil; M, clean-soil with metaschoepite (10%, w/w); M+Mn, metaschoepite (10%, w/w) combined with Mn(II)-chloride (2%, w/w). Same as below.

Dynamics of the in situ soil pH and Eh are presented in Fig. 1. During the incubation period, in both the saturation and flooding groups, the pH of soils decreased over the first 14 d, and then increased afterwards to approximately initial values (Fig. 1a, 1b). The addition of Mn(II)-salts resulted further decrease in pHs in comparison with the CK treatment. After 90 d of incubation, the pH of all soils reached a relatively steady state. Soil properties (such as pH, organic matter and cation exchange capacity) and flooding time were the main factors that controlled the change of soil pH after flooding. Similarly, Ding et al. found that the pH of soils with an initial pH > 6.5

were first decreased from 1 to 30 d and then increased afterwards to approximately 7.0 on average under the flooding period.[31] At the end of incubation, the order of soils pH in both groups was as follows: CK > M > M+Mn.

The soil Eh of all treatments was between 150 and 400 mV for the saturation group during the incubation period (Fig. 1c). Water regimes significantly altered the soil Eh. The Eh of soils in the flooding group were persistently decreased from 1 to 60 d. After, the soil Eh was then gradually increased to a stable stage, with ~50 mV level of all treatments in 270 d (Fig. 1d). Besides, the addition of Mn(II)-salts have no significant effect on the Eh of soils.

3.2 Dynamic changes of the soluble U and Mn

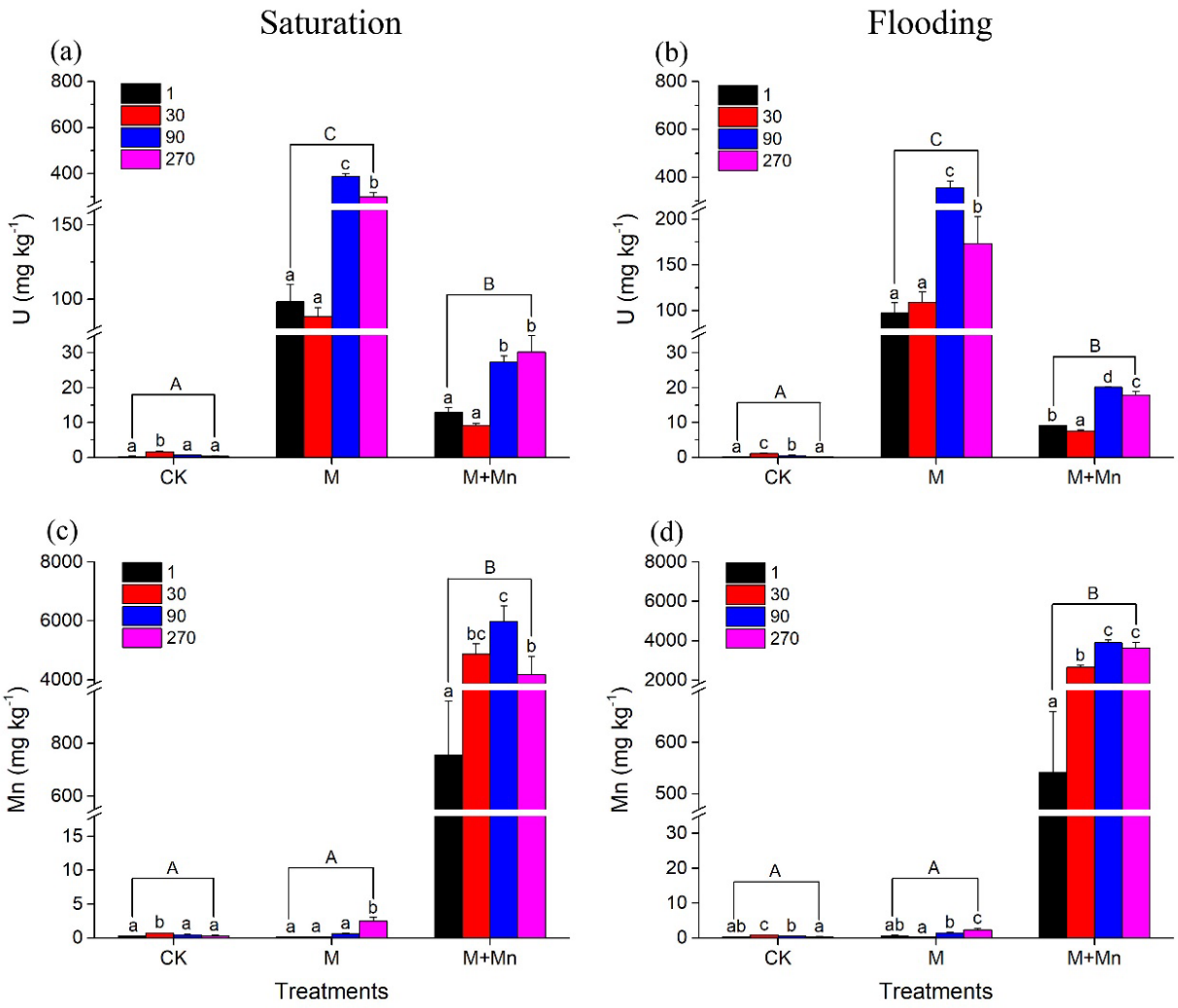

Fig 2. Dynamic changes of the water-extractable U and Mn during 270 d incubation. The different lowercase letters indicate significant differences between incubation days within same amendment treatments, and the different uppercase letters represent significant differences between amendment treatments.

Dynamic changes of the water-extractable U and Mn are shown in Fig. 2. The soluble U and Mn in soils were significantly affected by amendments, incubation days and their interaction. During the incubation period, the water-extractable U and Mn concentrations in the clean-soil (CK treatment) for both the saturation and flooding groups were slightly increased at the beginning and then return to their initial level. The spiking of metaschoepite significantly increased the concentrations of water-extractable U in soils, however, negligible changes of water-extractable

Mn in soils were found, while the releasing of Mn from metaschoepite were observed in the water system (Fig. S3). At the end of incubation (270 d), the concentrations of water-extractable U in the metaschoepite-amended soils (M treatment) for the saturation and flooding groups were 299 and 173 mg kg^{-1}, respectively (Fig. 2a, 2b). The addition of Mn(II)-chloride persistently increased the concentrations of water-extractable Mn in soils. After 270 d incubation, the concentrations of water-extractable Mn in the M+Mn treatments for the saturation and flooding groups were 4169 and 3644 mg kg^{-1}, respectively (Fig. 2c, 2d).

3.3 Characterization of metaschoepite transformation

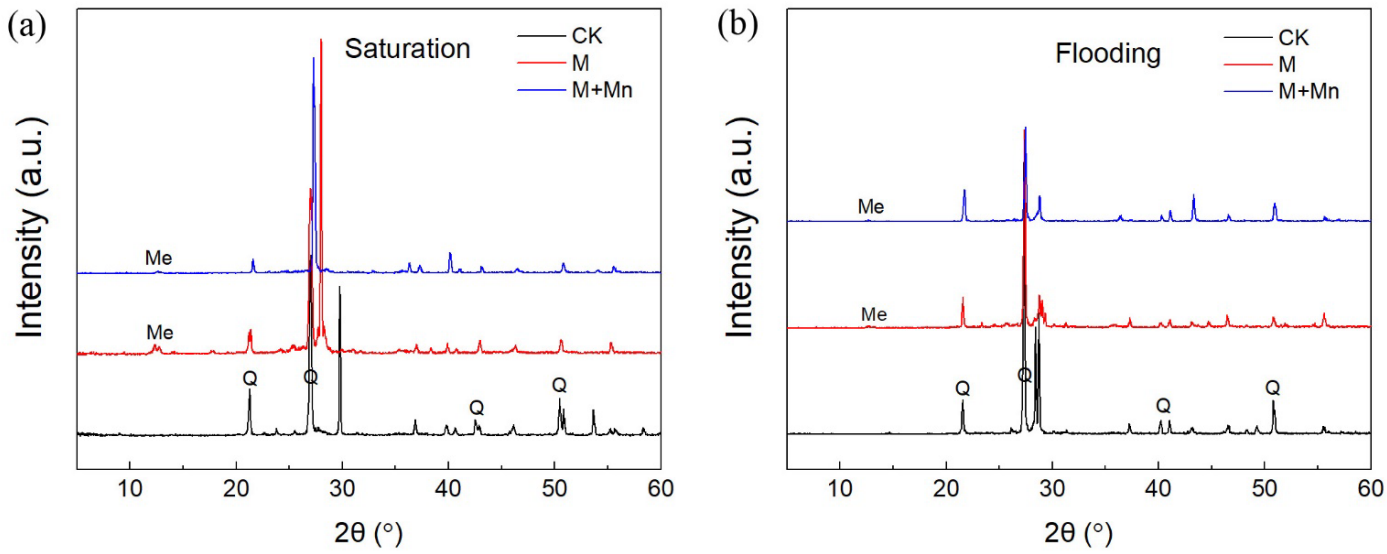

Fig 3. The XRD patterns of the metaschoepite-amended soils after 270 d incubation under saturation (a) and flooding (b) conditions. Me, metaschoepite; Q, quartz.

After 270 days, the XRD was used to evaluate mineral changes in metaschoepite-amended soils within the 4 experimental conditions (Fig. 3). Weak peaks that matched the major reflections of crystalline metaschoepite were observed in metaschoepite-amended soils. The diffraction peaks located at 12.01°(002) and 12.15°(021) were observed and attributed to UO_2 (JCPDS#13-0407) or $(UO_2)_8O_2(OH)_{12}\cdot 10H_2O$ (JCPDS#89-7333). An absence of diffraction peaks characteristic of

metaschoepite was noted in M+Mn treatments. Besides, for the soil amended with metaschoepite only (M treatments), the signals of metaschoepite in the flooding group were weakened in comparison to those in the saturation group (Fig. 3b). Changes in the XRD patterns of metaschoepite in the water system (Fig. S4) showed that the minor component becquerelite ($Ca(UO_2)_6O_4(OH)_6 \cdot 8H_2O$, JCPDS#39-0516) in DU corroded-product spiking material disappeared over the course of the experiment. The transformation of U(VI) minerals in DU corroded-products would increase the overall solubility of uranium in soil.[8, 29]

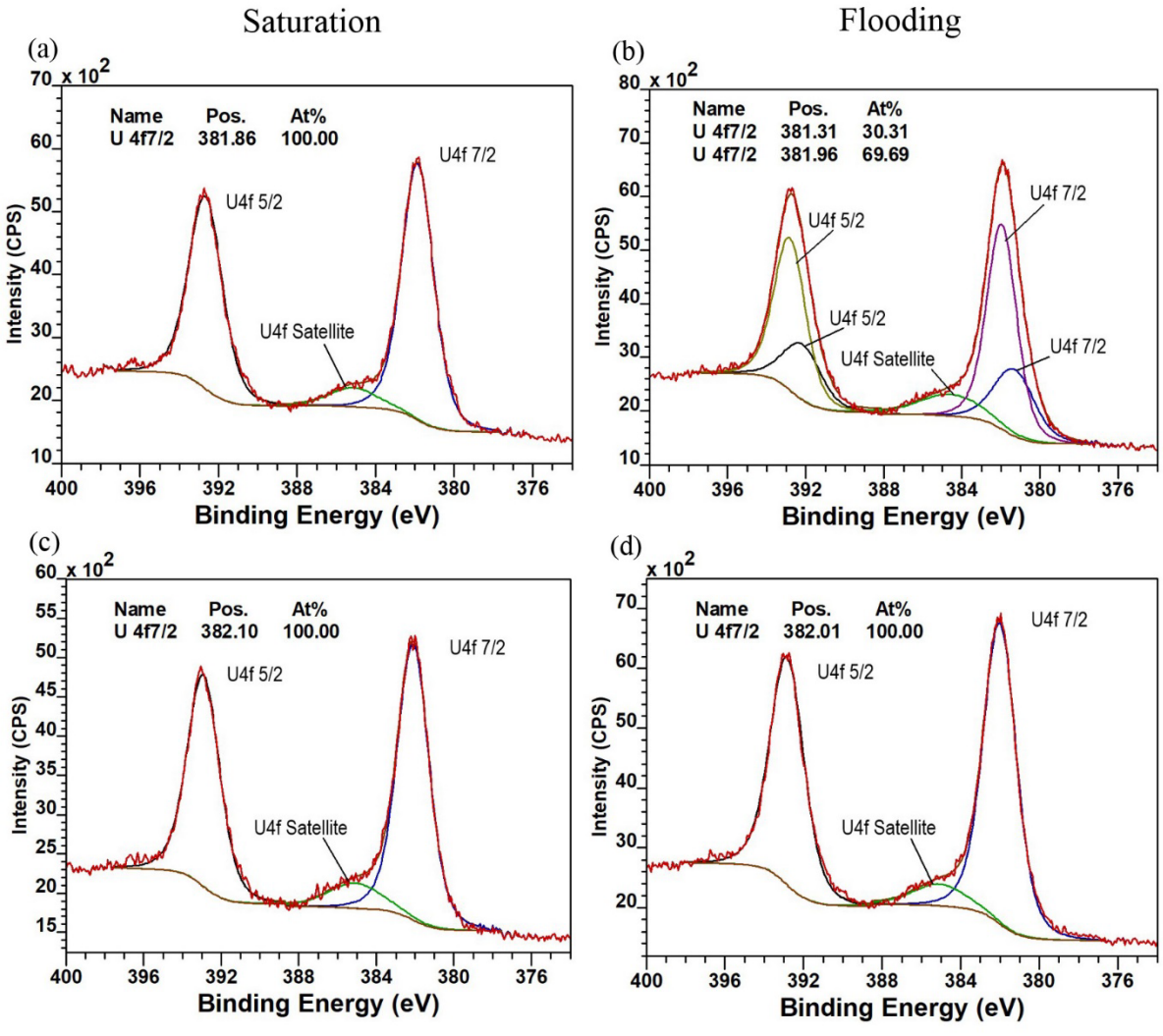

Fig 4. The XPS spectra of U after 270 d incubation under saturation (a, c) and flooding (b, d) conditions in the M (a, b) and M+Mn (c, d) treatments.

The XPS U(4f) spectra of metaschoepite-amended soils are shown in Fig. 4. The U4f7/2 spectrum consists of two components with binding energy levels of approximately 381.3 and 382.0 eV, both annotated as U(VI) in the metaschoepite-amended soil (M treatment) of the flooding group (Fig. 4b). And a satellite at a 4f7/2 peak with spacing of 3.7 eV from the primary peak were also assigned to U(VI).[34] Quantitatively, the XPS results indicated that U(VI) was the dominant species of liberated uranium in metaschoepite-amended soils in both the saturation and flooding group, moreover, the addition of Mn(II)-salts have no detectable effects on the reduction of U(VI) released from the metaschoepite in soil. However, the U4f7/2 spectrum with three components with binding energy levels of approximately 382.3, 381.1 and 379.8 eV, annotated as U(VI), U(V) and U(IV)[20] which might be related to low redox potential in the flooded system as noted in the Fig. 1, were found in metaschoepite under flooding treatment in water system (Fig. S5).

The Mn(2p) spectra for Mn(II)-treated metaschoepite-amended soils showed that the presence of Mn2p3/2 peaks at ~642.3 eV (Fig. 5), which correspond to the binding energy of Mn(III).[35] And no obvious shape difference between the saturation group and the flooding group was observed for the Mn(2p) spectra.

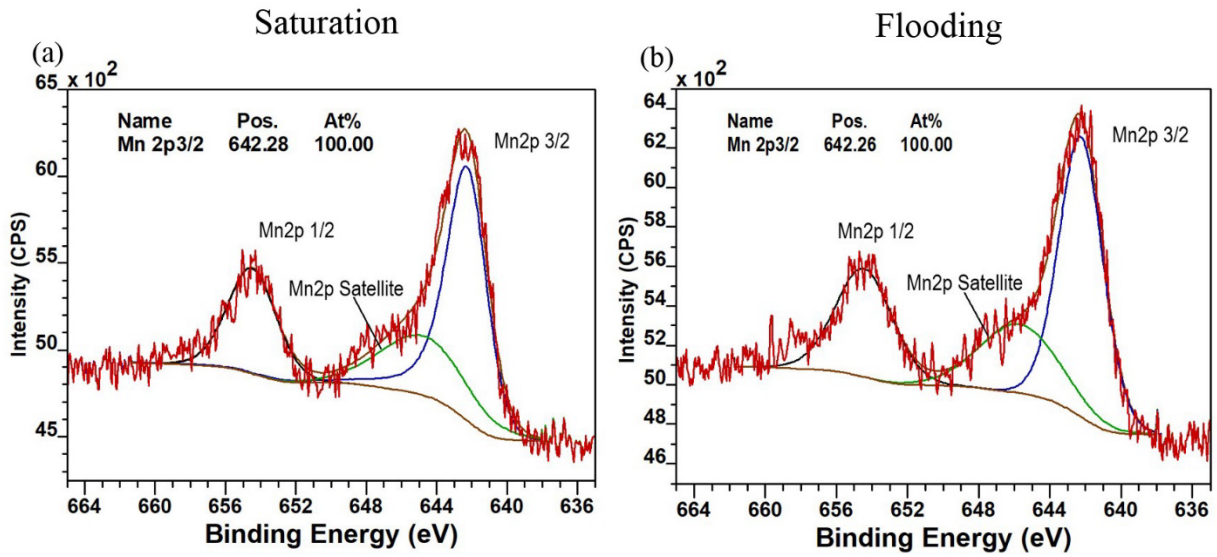

Fig 5. The XPS spectra of Mn after 270 d incubation under saturation (a) and flooding (b) conditions in the M+Mn treatments.

3.4 Stabilization effects of water regimes on metaschoepite

Metaschoepite is a primary product of DU munition corrosion in former war zones and at military test sites, which is important reservoir of mobile uranium in the environment and the release of UO_2^{2+} occurred with the dissolution of metaschoepite.

In the present study, at the beginning (1-90 d), both water regimes showed no significant effect on the concentrations of water-extractable U in the metaschoepite-amended soils, while the amounts of water extractable U were significantly reduced in the flooded group in the last 180 days of incubation period (Fig. 2). However, the releasing of U from metaschoepite was persistently inhibited by water regimes in water system (Fig. S3) since more anoxic condition was progressively formed in the flooding group (Fig. S5), and the redox reduction of U(VI) to U(V) and U(IV) in metaschoepite was found in water system. A column experiment investigated the transport of metaschoepite ($(UO_2)_8O_2(OH)_{12}\cdot 10H_2O$) over 98 days in sand-rich environments.[27] Majority of released U from metaschoepite were sorbed to the sand in a chemical fraction with

slow desorption, and the transportation of metaschoepite in sand was mainly depends on its dissolution and the interaction of dissolved UO_2^{2+} with the sand particles. Bower et al. investigated the dissolution of synthetic metaschoepite ($UO_3 \cdot 1.3H_2O$) and the biogeochemistry of liberated U in complex sediment/groundwater systems.[14] In the oxic columns, metaschoepite dissolution resulted in significant U(VI) transport, while the reaction with iron-containing sediment species retarded uranium migration; in the electron-donor amended columns (1 mmol L^{-1} of acetate/lactate 50:50 was added), U(VI), noncrystalline U(IV), and UO_2 were all observed in the sediment. The study confirmed the transformation of liberated U(VI) in metaschoepite amended-soils to U(IV) colloid under reducing condition. The present study showed that the dissolution and transformation of metaschoepite were controlled by water status and redox processes in both soil and water systems, which have great potential in the application of stabilizing the liberated U and its migration in the immediate proximity of DU deposited region.

3.5 Stabilization effects of Mn(II)-salts on metaschoepite

In the present study, Mn(II)-salts significantly retarded the amount of water extractable U from the soil containing metaschoepite (Fig. 2), though no detectable reduction of U(VI) was observed (Fig. 4). As reported, the introduction of Mn(II) (such as $MnCl_2$) into microoxic or oxygenated subsurface regions may provide conditions ideal for biological oxidation of Mn and formation of Mn oxides.[36] Mn(II) oxidation and in situ formation of Mn oxides may serve as a potential remediation strategy for U-contaminated groundwater since Mn(II) retention of U(VI) via strong adsorption.[23] This may be also supported by the results of XPS that no detectable U (VI) reduction was observed in the metaschoepite-amended soils with Mn(II) (Fig. 4). Ligand-stabilized Mn(III) species was recently recognized as an important redox-active intermediate in Mn biogeochemical cycling, and also in UO_2 dissolution.[37] Mn(II)-salts persistently reduced the amounts of water

extractable U in metaschoepite-amended soils, with only 10% of the water extractable U observed compared to the soil containing metaschoepite alone, > 90% of U stabilized during 270 d incubation (Fig. 6). Concurrent with the reduction of U solubility was the oxidations of Mn(II) to Mn(III) (Fig. 5). Irrespective of the mechanisms, significantly stabilization effect of Mn(II)-salts on metaschoepite dissolution and transformation, and the solubility of liberated U(VI) under both the saturation and flooding condition in soil as observed in this study was novel and additional work is now required to underpin a mechanistic understanding of their formation.

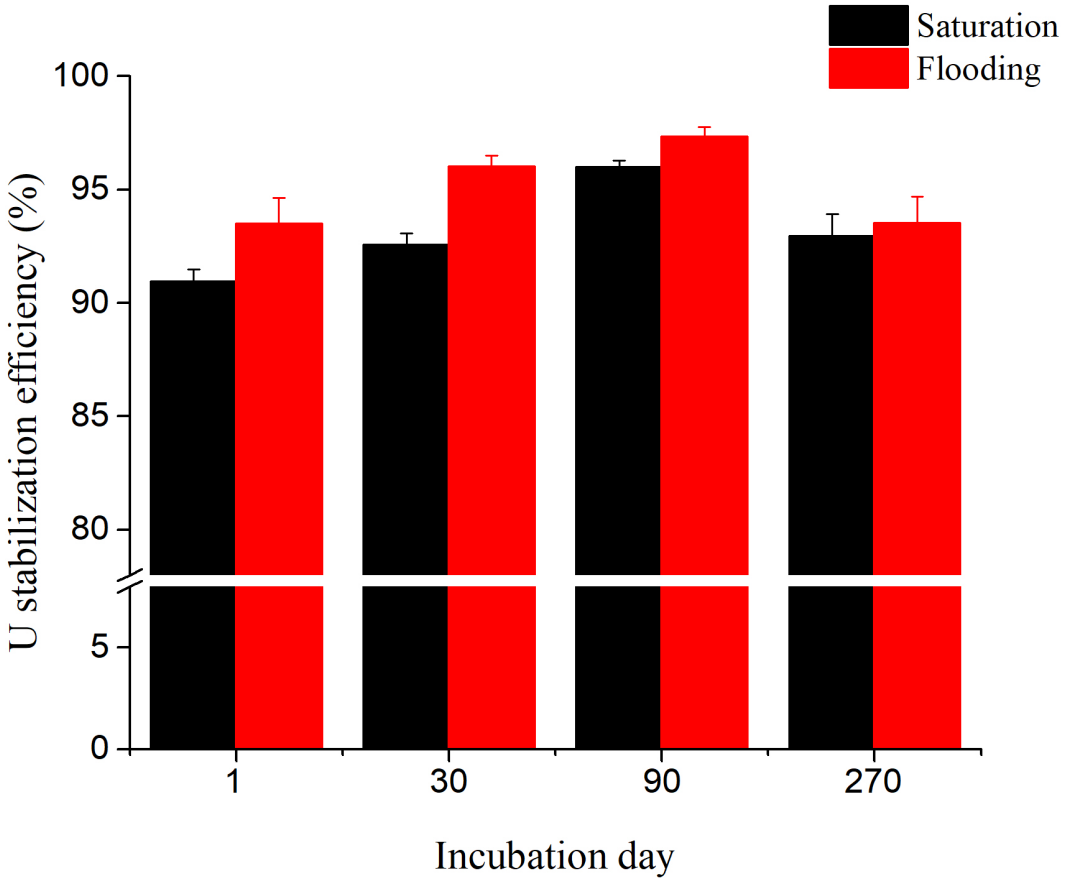

Fig 6. The dynamic changes of U stabilization efficiency as affected by Mn-salts.

4. ENVIRONMENTAL IMPLICATIONS

313 Wars or military testing have left a legacy of DU penetrators waste in terrestrial and marine
314 environments, however, very little information was available on the fate of DU penetrators
315 corrosion products in environmental systems. Recently, we have investigated the spatial
316 distribution and U fractionation in weapon testing sites and corrosion of DU under the
317 biogeochemical conditions-soil moistures.[3,10] Understanding the behavior and, in particular, the
318 dissolution and transformation of DU-corroded products metaschoepite in the vicinity of test-firing
319 sites is therefore of great importance. Generally, natural or constructed wetlands were applied for
320 the remediation of uranium-contaminated water based on redox reduction of U(VI).[38] Further,
321 shallow or deep disposal were usually used in the management of metaschoepite-bearing wastes[14]
322 and chemical leaching was applied to remediate DU-contaminated soils.[39] The present study
323 provided a simple method using the Mn(II)-salts as the stabilization agents which have great
324 potential in practical application for in-situ remediation of U-contaminated sites.

325 ## 5. CONCLUSIONS

326 The current work has shown that the water regimes and Mn(II)-salts addition significantly affected
327 the U liberation and its fate in soil system during metaschoepite dissolution and transformation.
328 No detectable reduction of U(VI) was observed in the "open waterlogged" soil system, while the
329 U stabilization efficiency of Mn(II) were > 90% in metaschoepite-amended soils, irrespective of
330 water regimes. The present study highlighted Mn(II)-salts is an excellent stabilizing amendment
331 of U(VI), which have potential in practical application for in-situ stabilization of U-contaminated
332 sites and nuclear waste disposal. In the future, the effects of Mn(II)-salts species on the
333 stabilization effectiveness need to be further investigated and the application dosage of Mn(II)-
334 salts need to be determined according to the actual soil condition since small amounts of Mn(II)
335 sustained the coupled redox processes of Mn.

6. ACKNOWLEDGMENTS

This study was supported by the U.S. Army Engineer Research and Development Center (W912HZ-16-2-0021), the U.S. Nuclear Regulatory Commission (NRC-HQ-84-15-G-0042, NRC-HQ-12-G-38-0038, NRC-HQ-84-16-G-0040) and the U.S. Department of Commerce (NOAA) NA11SEC4810001-003499, NA16SEC4810009, NOAA Center for Coastal and Marine Ecosystems Grant # G634C22

REFERENCES

(1) WHO, Depleted Uranium: Sources, Exposure and Health Effects. *Geneva, Switzerland* **2001**.
(2) Bleise, A.; Danesi, P. R.; Burkart, W., Properties, use and health effects of depleted uranium (DU)：a general overview. *Journal of environmental radioactivity* **2003,** *64*, 93-112.
(3) Kazery, J. A.; Proctor, G.; Larson, S. L.; Ballard, J. H.; Knotek-Smith, H. M.; Zhang, Q. K.; Celik, A.; Dasari, S.; Islam, S. M.; Tchounwou, P. B.; Han, F. X., Distribution and Fractionation of Uranium in Weapon Tested Range Soils. *ACS Earth and Space Chemistry* **2021,** *5*, (2), 356-364.
(4) Proctor, G.; Wang, H.R.; Larson, S. L.; Ballard, J. H.; Knotek-Smith, H.; Waggonor, C.; Unz, R.; Li, J. X.; McComb, J.; Jin, D. C.; Arslan, Z.; Han, F. X., Rapid Screening for Uranium in Soils Using Field-Portable X-ray Fluorescence Spectrometer: A Comparative Study. *ACS Earth and Space Chemistry* **2020,** *4*, (2), 211-217.
(5) Handley-Sidhu, S.; Keith-Roach, M. J.; Lloyd, J. R.; Vaughan, D. J., A review of the environmental corrosion, fate and bioavailability of munitions grade depleted uranium. *The Science of the total environment* **2010,** *408*, (23), 5690-700.
(6) Lind, O. C.; Tschiersch, J.; Salbu, B., Nanometer-micrometer sized depleted uranium (DU) particles in the environment. *Journal of environmental radioactivity* **2020,** *211*, 106077.
(7) Sowder, A. G.; Clark, S. B.; Fjeld, R. A., The Transformation of Uranyl Oxide Hydrates: The Effect of Dehydration on Synthetic Metaschoepite and Its Alteration to Becquerelite. *Environmental science and technology* **1999,** *33*, 3552-3557.
(8) Wang, Y.; von Gunten, K.; Bartova, B.; Meisser, N.; Astner, M.; Burger, M.; Bernier-Latmani, R., Products of in Situ Corrosion of Depleted Uranium Ammunition in Bosnia and Herzegovina Soils. *Environmental science and technology* **2016,** *50*, (22), 12266-12274.
(9) Buck, B. J.; Brock, A. L.; Johnson, W. H.; Ulery, A. L., Corrosion of Depleted Uranium in an Arid Environment: Soil-Geomorphology, SEM/EDS, XRD, and Electron Microprobe Analyses. *Soil and Sediment Contamination* **2004,** *13*, (6), 545-561.
(10) Zhang, Q. K.; Larson, S. L.; Ballard, J. H.; Zhu, X. C.; Knotek-Smith, H. M.; Han, F. X., Uranium metal corrosion in soils with different soil moisture regimes. *Corrosion Science* **2021,** *179*, 109138.
(11) Handley-Sidhu, S.; Worsfold, P. J.; Livens, F. R.; Vaughan, D. J.; Lloyd, J. R.; Boothman, C.; Sajih, M.; Alvarez, R.; Keith-Roach, M. J., Biogeochemical Controls on the Corrosion

of Depleted Uranium Alloy in Subsurface Soils. *Environmental Science and Technology* **2009,** *43*, 6177-6182.
(12) Alessi, D. S.; Uster, B.; Veeramani, H.; Suvorova, E. I.; Lezama-Pacheco, J. S.; Stubbs, J. E.; Bargar, J. R.; Bernier-Latmani, R., Quantitative separation of monomeric U(IV) from UO_2 in products of U(VI) reduction. *Environmental science and technology* **2012,** *46*, (11), 6150-7.
(13) Baker, M. R.; Coutelot, F. M.; Seaman, J. C., Phosphate amendments for chemical immobilization of uranium in contaminated soil. *Environment international* **2019,** *129*, 565-572.
(14) Bower, W. R.; Morris, K.; Livens, F. R.; Mosselmans, J. F. W.; Fallon, C. M.; Fuller, A. J.; Natrajan, L.; Boothman, C.; Lloyd, J. R.; Utsunomiya, S.; Grolimund, D.; Ferreira Sanchez, D.; Jilbert, T.; Parker, J.; Neill, T. S.; Law, G. T. W., Metaschoepite Dissolution in Sediment Column Systems-Implications for Uranium Speciation and Transport. *Environmental science and technology* **2019**.
(15) Meng, F. D.; Jin, D. C.; Guo, K.; Larson, S. L.; Ballard, J. H.; Chen, L. M.; Arslan, Z.; Yuan, G. D.; White, J. R.; Zhou, L. X.; Ma, Y. H.; Waggoner, C. A.; Han, F. X., Influences of U Sources and Forms on Its Bioaccumulation in Indian Mustard and Sunflower. *Water, Air, and Soil Pollution* **2018,** *229*, (11).
(16) Wall, J. D.; Krumholz, L. R., Uranium reduction. *Annual review of microbiology* **2006,** *60*, 149-66.
(17) UNEP, Depleted Uranium in Bosnia and Herzegovina: Post-Conflict Environmental Assessment. *Geneva, Switzerland* **2003**.
(18) Lovley, D. R.; Phillips, E. J. P.; Gorby, Y. A.; Landa, E. R., Microbial Reduction of Uranium. *Nature* **1991,** *350*, 413-416.
(19) Duan, J.; Ji, H. D.; Liu, W.; Zhao, X.; Han, B.; Tian, S. T.; Zhao, D. Y., Enhanced immobilization of U(VI) using a new type of FeS-modified Fe^0 core-shell particles. *Chemical Engineering Journal* **2019,** *359*, 1617-1628.
(20) Xie, Y. P.; Fang, Q.; Li, M.; Wang, S. N.; Luo, Y. F.; Wu, X. Y.; Lv, J. W.; Tan, W. F.; Wang, H. Q.; Tan, K. X., Low concentration of Fe(II) to enhance the precipitation of U(VI) under neutral oxygen-rich conditions. *The Science of the total environment* **2020,** *711*, 134827.
(21) Tebo, B. M.; Bargar, J. R.; Clement, B. G.; Dick, G. J.; Murray, K. J.; Parker, D.; Verity, R.; Webb, S. M., BIOGENIC MANGANESE OXIDES: Properties and Mechanisms of Formation. *Annual Review of Earth and Planetary Sciences* **2004,** *32*, (1), 287-328.
(22) Wang, Z. M.; Lee, S. W.; Kapoor, P.; Tebo, B. M.; Giammar, D. E., Uraninite oxidation and dissolution induced by manganese oxide: A redox reaction between two insoluble minerals. *Geochimica et Cosmochimica Acta* **2013,** *100*, 24-40.
(23) Wang, Z. M.; Lee, S. W.; Catalano, J. G.; Lezama-Pacheco, J. S.; Bargar, J. R.; Tebo, B. M.; Giammar, D. E., Adsorption of uranium(VI) to manganese oxides: X-ray absorption spectroscopy and surface complexation modeling. *Environmental science and technology* **2013,** *47*, (2), 850-8.
(24) Ren, Y. M.; Bao, H. L.; Wu, Q.; Wang, H. S.; Gai, T.; Shao, L.; Wang, S. F.; Tang, H.; Li, Y. R.; Wang, X. K., The physical chemistry of uranium (VI) immobilization on manganese oxides. *Journal of hazardous materials* **2020,** *391*, 122207.
(25) Lee, S. Y.; Cha, W. S.; Kim, J. G.; Baik, M. H.; Jung, E. C.; Jeong, J. T.; Kim, K.; Chung, S. Y.; Lee, Y. J., Uranium(IV) remobilization under sulfate reducing conditions. *Chemical Geology* **2014,** *370*, 40-48.

(26) Liu, C. X.; Zachara, J. M.; Fredrickson, J. K.; Kennedy, D. W.; Dohnalkova, A., Modeling the Inhibition of the Bacterial Reduction of U(VI) by β-MnO_2(s). *Environmental science and technology* **2002,** *36*, 1452-1459.
(27) Handley-Sidhu, S.; Bryan, N. D.; Worsfold, P. J.; Vaughan, D. J.; Livens, F. R.; Keith-Roach, M. J., Corrosion and transport of depleted uranium in sand-rich environments. *Chemosphere* **2009,** *77*, (10), 1434-9.
(28) Lind, O. C.; Salbu, B.; Skipperud, L.; Janssens, K.; Jaroszewicz, J.; De Nolf, W., Solid state speciation and potential bioavailability of depleted uranium particles from Kosovo and Kuwait. *Journal of environmental radioactivity* **2009,** *100*, (4), 301-7.
(29) Qader, M. A.; Kersten, M., Chronospeciation of uranium released in soil during a long-term DU shell weathering experiment. *Journal of environmental radioactivity* **2021,** *228*, 106511.
(30) Han, F. X.; Banin, A., Long-term transformations of cadmium, cobalt, copper, nickel, zinc, vanadium, manganese, and iron in arid-zone soils under saturated condition. *Communications in Soil Science and Plant Analysis* **2000,** *31*, (7-8), 943-957.
(31) Ding, C. F.; Du, S. Y.; Ma, Y. B.; Li, X. G.; Zhang, T. L.; Wang, X. X., Changes in the pH of paddy soils after flooding and drainage: Modeling and validation. *Geoderma* **2019,** *337*, 511-513.
(32) Chen, L. M.; Larson, S. L.; Ballard, J. H.; Ma, Y. H.; Zhang, Q. K.; Li, J. X.; Wu, L. C.; Arslan, Z.; Han, F. X., Laboratory spiking process of soil with various uranium and other heavy metals. *MethodsX* **2019,** *6*, 734-739.
(33) Rocha, L.; Rodrigues, S. M.; Lopes, I.; Soares, A. M.; Duarte, A. C.; Pereira, E., The water-soluble fraction of potentially toxic elements in contaminated soils: relationships between ecotoxicity, solubility and geochemical reactivity. *Chemosphere* **2011,** *84*, (10), 1495-505.
(34) Huber, F.; Schild, D.; Vitova, T.; Rothe, J.; Kirsch, R.; Schäfer, T., U(VI) removal kinetics in presence of synthetic magnetite nanoparticles. *Geochimica et Cosmochimica Acta* **2012,** *96*, 154-173.
(35) Ilton, E. S.; Post, J. E.; Heaney, P. J.; Ling, F. T.; Kerisit, S. N., XPS determination of Mn oxidation states in Mn (hydr)oxides. *Applied Surface Science* **2016,** *366*, 475-485.
(36) Wang, Z. M.; Tebo, B. M.; Giammar, D. E., Effects of Mn(II) on UO_2 dissolution under anoxic and oxic conditions. *Environmental science and technology* **2014,** *48*, (10), 5546-54.
(37) Wang, Z. M.; Xiong, W.; Tebo, B. M.; Giammar, D. E., Oxidative UO_2 dissolution induced by soluble Mn(III). *Environmental science and technology* **2014,** *48*, (1), 289-98.
(38) Dublet, G.; Worms, I.; Frutschi, M.; Brown, A.; Zund, G. C.; Bartova, B.; Slaveykova, V. I.; Bernier-Latmani, R., Colloidal Size and Redox State of Uranium Species in the Porewater of a Pristine Mountain Wetland. *Environmental science and technology* **2019**.
(39) Crean, D. E.; Livens, F. R.; Sajih, M.; Stennett, M. C.; Grolimund, D.; Borca, C. N.; Hyatt, N. C., Remediation of soils contaminated with particulate depleted uranium by multi stage chemical extraction. *Journal of hazardous materials* **2013,** *263*, 382-90.